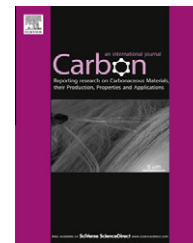


Available at [www.sciencedirect.com](http://www.sciencedirect.com)

SciVerse ScienceDirect

journal homepage: [www.elsevier.com/locate/carbon](http://www.elsevier.com/locate/carbon)

# A simple scheme of molecular electronic devices with multiwalled carbon nanotubes as the top electrodes

Jason P. Moscatello, Abhishek Prasad, Ravi Chintala, Yoke Khin Yap \*

Department of Physics, Michigan Technological University, 118 Fisher Hall, 1400 Townsend Drive, Houghton, MI 49931, USA

## ARTICLE INFO

### Article history:

Received 25 January 2012

Accepted 10 March 2012

Available online 19 March 2012

## ABSTRACT

A simple fabrication scheme for molecular electronic junctions is presented with multiwalled carbon nanotubes (MWCNTs) as the top electrodes. Results indicate that our approach retains the molecular character of the chosen molecules [a self-assembled monolayer of octadecanethiol on gold bottom electrodes] and opens the door for studying a wide variety of organothiol candidates for molecular electronics. The fabrication scheme is designed in a way that it can be modified into all-carbon devices in the future by using graphitic carbon bottom electrodes functionalized with nitrozoabenzene, for example, and MWCNTs or graphene as the top electrodes. Alternatively, the scheme is applicable for all-gold devices with gold bottom electrodes and gold nanowire top electrodes.

© 2012 Elsevier Ltd. All rights reserved.

## 1. Introduction

Molecules are the smallest possible switching elements for future electronic devices. While a great many types of devices are being considered, including those using nanowires and nanotubes as the active elements, the smallest possible devices will be those based on zero-dimensional molecules. One of the most important goals of such molecular electronics is to replace conventional CMOS components [1,2]. However, fabrication and wiring of these molecules, which are called *molecular junctions*, remains the most challenging aspect [2,3] of this research. In fact, most molecular electronic properties were demonstrated based on scanning tunneling microscopy (STM). Although the fundamental chemical and electronic properties of these molecules can be conveniently demonstrated by using STM, these properties may be altered by integration of these molecules into devices.

Molecular junctions reported thus far can be classified into two main categories. The first is *individual junctions* which are excellent for studies, but have the drawback that their design

does not make them compatible with formation into arrays of junctions. Examples include break junctions [4–6] and studies based on STM [7–9]. While the study of these individual junctions can offer good initial insights into the characteristics and behaviors of molecules, it is known that two very similar junctions can have different behavior due to fabrication differences [3,10,11]. In contrast, the second category is based on *arrays of junctions*, but these are extremely difficult or complicated to assemble and not necessarily reproducible by others [12].

In the present work, we fabricate molecular junctions using commonly available techniques that are readily reproducible by others. Because of the introduction of one dimensional (1D) materials (multiwalled carbon nanotubes, MWCNTs) as the top electrodes, the junctions are easily compatible with current nanoscale devices with nanowires and nanotubes, and thus scalable to arrays of molecular junctions. In addition, none of the character of the junctions is dependent on bulk properties, so they can be further scaled to smaller dimensions without losing the physics and chemistry that makes them unique.

\* Corresponding author: Fax: +1 906 487 2933.

E-mail address: [ykyap@mtu.edu](mailto:ykyap@mtu.edu) (Y.K. Yap).

0008-6223/\$ - see front matter © 2012 Elsevier Ltd. All rights reserved.

<http://dx.doi.org/10.1016/j.carbon.2012.03.021>

## 2. Experimental procedures

Our molecular junctions are prepared based on commonly available techniques such as photolithography of gold electrodes, self-assembled monolayers (SAMs) of organothiol molecules on these gold electrodes, and dielectrophoresis (DEP) of MWCNTs across these organothiol-gold electrodes. As schematically shown in Fig. 1a, arrays of patterned gold pads are first deposited on oxidized Si substrates as the bottom electrodes (Fig. 1b). After annealing, these gold electrodes are then functionalized with our organothiol SAM octadecanethiol (ODT) molecules on their surfaces (Fig. 1c). For the top electrodes, MWCNTs were subsequently deposited on these SAM molecules by DEP (Fig. 1d). MWCNTs are an ideal choice for top contacts because they are always conductive (semi-metallic), removing the need for post-growth sorting (which is necessary for single-walled CNTs). These MWCNTs are capable of forming stable contact with ODT without destroying the molecules, and they can be placed with DEP in order to build wired arrays. It should be noted that the studied junctions are double-junctions, meaning that the current must pass through the ODT molecules twice, once each at the surface of the gold/ODT bottom electrodes at both ends of the MWCNTs. This double junction scheme was chosen for speed of fabrication. A single junction can be made instead by making one of the two electrodes with a conductive material other than gold.

The molecular junction fabrication process is as follows. Substrates were p-type silicon with a 120 nm thick thermal

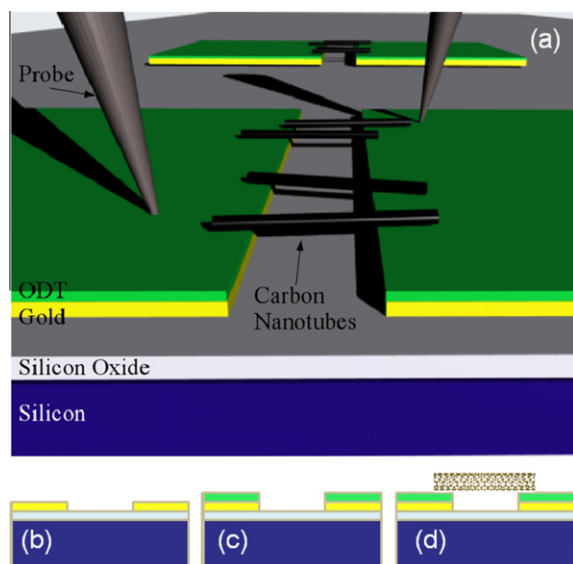


**Fig. 1 – (a) Schematic of our molecular junctions. The current flows through one probe tip to the gold (the tips penetrate through the ODT layer to the underlying gold), then through the ODT to one end of the MWCNTs. Once the current flows through the MWCNTs, it passes through the ODT to the gold and to the other probe tip. For speed of fabrication (b, c, d), such a double junction configuration (current passing ODTs at both ends MWCNTs) was made. A single junction configuration can easily be made instead by making one of the two electrodes non-gold.**

SiO<sub>2</sub> layer. The surfaces were first cleaned by ultrasonication in acetone followed by ethanol, and further cleaned with an Ar plasma in the sputtering chamber prior to the deposition of gold films. A gold film was deposited by plasma sputtering (Perkin-Elmer Randex Sputtering System Model 2400) to a thickness of 60 nm. The square patterns of the gold films were fabricated with traditional UV microphotolithography using Futurrex NR9G-1000PY photoresist in combination with a gold etchant step. Finally, the patterning was finished by removing residual resist by acetone and ethanol baths. Before SAM deposition, the gold was annealed; this is discussed in detail in the following section. After annealing, the gold electrodes were then functionalized with ODT by a self-assembly process where the substrates are immersed in a 2 mM ODT in ethanol solution inside a nitrogen environment glovebox for 48 h. Upon removal from solution, the substrates are rinsed thoroughly in a stream of ethanol to make sure no residual ODT contaminates the surface. Dielectrophoretic deposition of MWCNTs between the electrodes completes the junctions.

## 3. Results and discussion

A series of annealing conditions were systematically investigated to flatten the surface of the as-deposited gold films and enhance their adhesion to the SiO<sub>2</sub> surface. This is important to form a uniform SAM on the gold electrodes. The root-mean-square (rms) roughness of the gold films was determined by atomic force microscopy (AFM, Veeco Dimension 3000) analysis at various scan areas (0.5 μm × 0.5 μm, 1 μm × 1 μm, 5 μm × 5 μm). As shown in Table 1, all samples acquired lower rms roughness after annealing for three hours. The optimum annealing conditions are 300 °C for 3 h in vacuum: the rms roughness is below 0.5 nm, more than suitable for quality SAM formation. In Fig. 2, the AFM images of the gold films after annealing at 200 °C and 300 °C are shown for comparison. As shown, the gold films annealed at 300 °C are much smoother with larger island sizes. Such a smooth surface morphology is important for SAMs of ODT with minimum defects.

ODT was chosen as our molecules because it is a robust organothiol with a large HOMO–LUMO gap (~6.033 eV) and should behave as an insulator [13,14] under low bias potential, making it a good test of our process. The expected shape of the I–V curve for ODT is like that reported by Labonté et al. [13] and confirmed by our own ambient STM study of SAM ODT on Au (Fig. 3a). As shown, the STM signal on ODT has (1) a well defined bias region (about ± 2 V) of extremely low current flow (~0.05 nA) centered symmetrically around 0 V, and (2) outside the low current region, current should begin to rapidly rise. We further compare this STM signal with that measured from a bare gold film. As shown in Fig. 3b, the STM current level is much higher for the gold films without ODT and the range of bias voltage at near zero current level is very narrow but not ignorable due to the tunneling barrier between the STM tip and the gold film.

The devices were completed by connecting the ODT coated gold electrodes (ODT/Au) with MWCNTs, by our surfactant-free DEP technique. The MWCNTs were grown by a thermal CVD process on a SiO<sub>2</sub> surface [15,16]. Surfactant-free DEP

**Table 1 – Root-mean-square roughness (in nanometers) of the gold films after annealing.**

Annealing conditions	rms (in nm) within $5 \mu\text{m} \times 5 \mu\text{m}$	rms (in nm) within $1 \mu\text{m} \times 1 \mu\text{m}$	rms (in nm) within $0.5 \mu\text{m} \times 0.5 \mu\text{m}$
As deposited	$0.8908 \pm 0.1438$	$0.7834 \pm 0.1127$	$0.7090 \pm 0.1104$
200 °C, 1 h	$0.7394 \pm 0.5350$	$0.6340 \pm 0.0140$	$0.6360 \pm 0.0260$
200 °C, 3 h	$0.6219 \pm 0.0099$	$0.5828 \pm 0.0159$	$0.5848 \pm 0.0255$
200 °C, 5 h	$0.8020 \pm 0.0180$	$0.7610 \pm 0.0244$	$0.7662 \pm 0.0241$
300 °C, 1 h	$0.6118 \pm 0.0715$	$0.5332 \pm 0.0337$	$0.5394 \pm 0.0275$
300 °C, 3 h	$0.5812 \pm 0.1619$	$0.4272 \pm 0.0139$	$0.4324 \pm 0.0129$
300 °C, 5 h	$0.6222 \pm 0.0174$	$0.5940 \pm 0.0300$	$0.5974 \pm 0.0387$
500 °C		Damaged*	

\* The numbers are unrounded figures.

\*\* The film was no longer covering the surface completely.

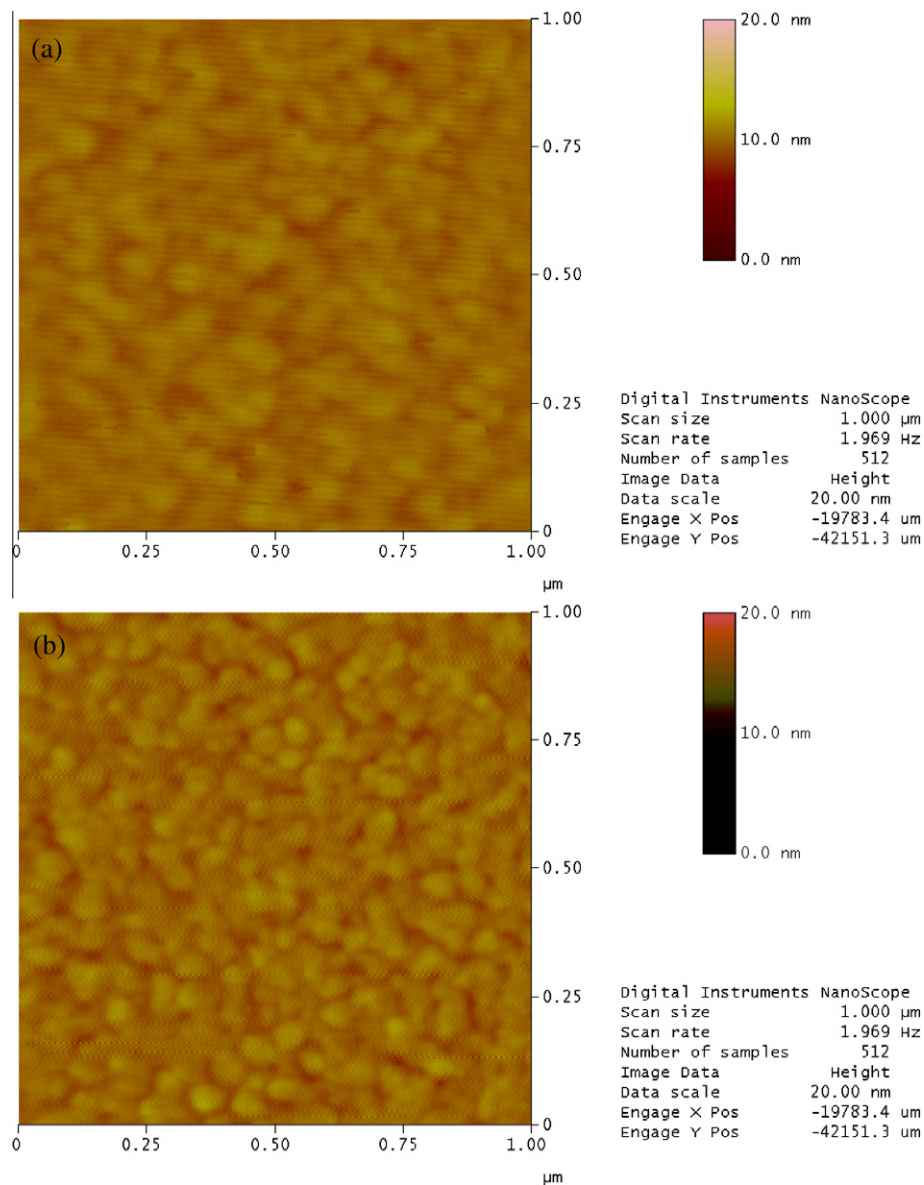


**Fig. 2 – AFM images of gold films after annealing for three hours in vacuum at (a) 300 °C and (b) 200 °C. Case (a) produces much smoother surfaces than case (b).**

was performed as described previously [17]. Briefly, the as-grown MWCNTs were removed from the substrates and

placed in ethanol without the use of surfactants. After optimum ultrasonication (2 h), a drop of the ethanol-MWCNT

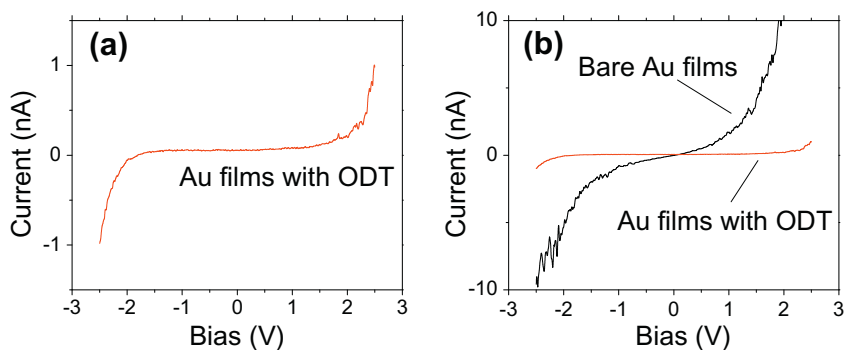


**Fig. 3 – (a) The I–V for Au with ODT shows the predicted insulated region centered around 0 V; outside of this region, current begins to rise rapidly. (b) Comparison of I–V taken with STM of Au films with and without ODT monolayers. When ODT is present, the current is greatly reduced versus pure Au at all voltages.**

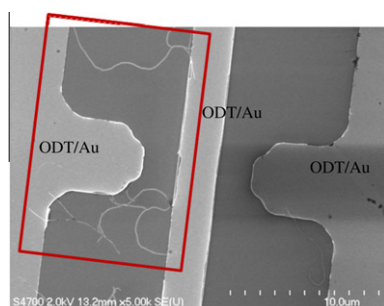


**Fig. 4 – Images of MWCNTs across the gap of two ODT coated gold (ODT/Au) electrodes. The boxed area shows part of the active region, where multiple MWCNTs are detected.**

suspension (5  $\mu\text{L}$ ) is placed over the microelectrode gap while a sinusoidal AC voltage at 30  $V_{pp}$  and 2 kHz is applied between them. The AC field causes the MWCNTs to align between the electrodes, spanning the gap between them and completing the device. Once completed, the junctions were tested using a Keithley 4200 SCS. An example of a completed device is shown in Fig. 4.

Molecular junctions fabricated using this technique show one of two types of current–voltage (I–V) characteristics as shown in Fig. 5. Fig. 5a shows the case where MWCNTs are shorted to the gold electrodes. In this case, the current flow is able to avoid the ODT layer altogether with current level five orders of magnitude (mA level) higher than that for molecular junctions (tens of nA level). The linear I–V behavior also suggests that MWCNTs deposited by DEP can form good contact with the gold electrodes. The short circuit shown here can take place by contacting an area of the gold where the ODT layer is incomplete, which is most likely to occur on the edge of the microelectrode. On the other hand, we also found some of the tested junctions exhibited the expected I–V molecular junctions with the fingerprint of ODT: a region of very low current flow centered on 0 V, outside of which the current begins to rise rapidly and non-linearly as shown in Fig. 5b. As shown, the I–V characters are reproducible as we scan the bias from 5 V to  $-5$  V (as guided by the downward red arrows) and then from  $-5$  V to 5 V (as guided by the upward blue arrows). In general, we found that such molecular I–V behavior was

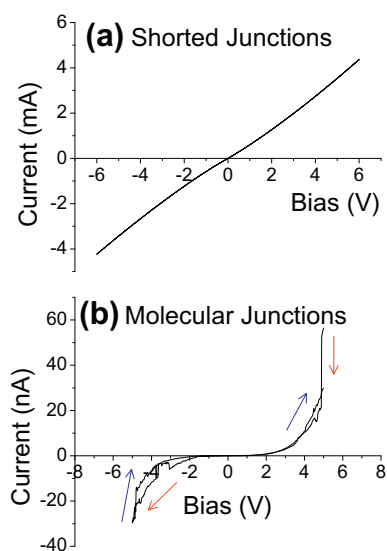


**Fig. 5 – Two types of current–voltage (I–V) characteristics detected from our devices. Note that the current scale differs between the plots. (a) Shorted junctions where MWCNTs have avoided ODT and are in contact with the gold electrodes. (b) Molecular junctions where MWCNTs are in contact with the ODT/Au electrodes. Repeatable scans can be reproduced as shown (see text for description).**

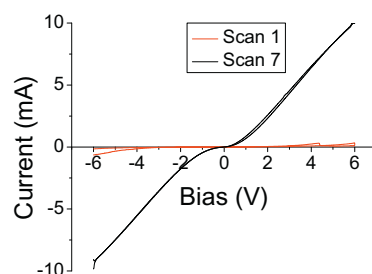


**Fig. 6 – Comparison of an ODT molecular junction's I–V behavior during the first and seventh voltage sweeps between +6 and  $-6$  V. After seven sweeps the resistance is much lower, and the current gap region's width has shrunk significantly.**

stable and repeatable within the low bias region (about  $\pm 4$  or  $\pm 5$  V). However, when ramping the bias voltages to values larger than about  $\pm 6$  V the current becomes unstable as shown in Fig. 6. As shown, the current level for seventh  $\pm 6$  V scan is much larger than the first, and approaching that of the shorted case shown in Fig. 5a. This result indicates that the ODT films sandwiched between MWCNTs and the gold pads deteriorate most likely due to Joule heating during the tests. All these data are representable results obtained from more than three devices.

#### 4. Summary

We have demonstrated a simple scheme for molecular electronic devices based on commonly used techniques, namely dielectrophoresis, UV photolithography, self-assembly monolayer, and annealing. Results indicate that our approach retains the molecular character of the chosen molecules (ODT in this case), opening up the door for studying a wide variety of candidates for molecular electronic devices. For example, one may replace the gold electrodes with graphic carbon electrodes and covalently functionalize with nitrozoabenzene [18]. With the MWCNT top electrodes shown here (or graphene top electrodes, which may be tested in the future), this will lead to all-carbon molecular electronic devices. In addition, our scheme is general for any organothiol, and is even more general if we replace the MWCNT top electrodes to Au nanowires that are functionalized with organothio molecules, for example. In this case, the microelectrode can be generalized to gold and lead to all-gold devices or any metallic materials.

#### Acknowledgments

This work is supported by Defense Advanced Research Projects Agency (Contract No.: DAAD17-03-C-0115, through Army Research Laboratory) and The Multi-Scale Technologies Institute (MuSTI) at Michigan Technological University. We thank Kumar Vanga, Dr. Karl Walczak and Dr. Chee Huei Lee of Michigan Technological University for their assistance.

#### REFERENCES

- [1] Heath JR. Molecular electronics. *Annu Rev Mater Res* 2009;39:1–23.
- [2] Akkerman HB, Blom PWM, de Leeuw DM, de Boer B. Towards molecular electronics with large-area molecular junctions. *Nature* 2006;441:69–72.
- [3] McCreery RL, Bergren AJ. Progress with molecular electronics junctions: meeting experimental challenges in design and fabrication. *Adv Mat* 2009;21(43):4303–22.
- [4] Reed MA, Zhou C, Muller CJ, Burgin TP, Tour JM. Conductance of a molecular junction. *Science* 1997;278(5336):252–4.
- [5] Hines T, Diez-Perez I, Hihath J, Liu H, Wang Z-S, Zhao J, et al. Transition from tunneling to hopping in single molecular junctions by measuring length and temperature dependence. *J Am Chem Soc* 2010;132(33):11658–64.
- [6] Yamada R, Kumazawa H, Noutoshi T, Tanaka S, Tada H. Electrical conductance of oligothiophene molecular wires. *Nano Lett* 2008;8(4):1237–40.
- [7] Haiss W, Nichols RJ, van Zalinge H, Higgins SJ, Bethell D, Schiffrin DJ. Measurement of single molecule conductivity using the spontaneous formation of molecular wires. *Phys Chem Chem Phys* 2004;6:4330–7.
- [8] Zhou J, Chen G, Xu B. Probing the molecule-electrode interface of single molecule junctions by controllable mechanical modulations. *J Phys Chem C* 2010;114(18):8587–92.
- [9] Seo K, Konchenko AV, Lee J, Bang GS, Lee H. Molecular conductance switch-on of single ruthenium complex molecules. *J Am Chem Soc* 2008;130(8):2553–9.
- [10] Tao NJ. Electron transport in molecular junctions. *Nature Nanotechnol* 2006;1:173–81.
- [11] Jin Y, Friedman N, Sheves M, Cahen D. Effect of metal-molecule contact roughness on electronic transport: bacteriorhodopsin-based, metal-insulator-metal planar junctions. *Langmuir* 2008;24(10):5622–6.
- [12] Collier CP, Mattersteig G, Wong EW, Luo Y, Beverly K, Sampaio J, et al. A [2]catenane-based solid state electronically reconfigurable switch. *Science* 2000;289(5482):1172–5.
- [13] Labonté AP, Tripp SL, Reifengerger R, Wei A. Scanning tunneling spectroscopy of insulating self-assembled monolayers on Au(111). *J Phys Chem. B* 2002;106(34):8721–5.
- [14] Kolipaka S, Aithal RK, Kuila D. Fabrication and characterization of an indium tin oxide-octadecanethiol-aluminum junction for molecular electronics. *Appl Phys Lett* 2006;88(23):233104.
- [15] Kayastha V, Yap YK, Dimovski S, Gogotsi Y. Controlling dissociative adsorption for effective growth of carbon nanotubes. *Appl Phys Lett* 2004;85(15):3265–7.
- [16] Moscatello JP, Wang J, Ulmen B, Mensah SL, Xie M, Wu S, et al. Controlled growth of carbon, boron nitride, and zinc oxide nanotubes. *IEEE Sensors Journal* 2008;8(6):922–9.
- [17] Moscatello J, Kayastha V, Ulmen B, Pandey A, Wu S, Singh A, et al. Surfactant-free dielectrophoretic deposition of multi-walled carbon nanotubes with tunable deposition density. *Carbon* 2010;48(12):3559–69.
- [18] McCreery RL, Wu J, Kalakodimi RP. Electron transport and redox reaction in carbon-based molecular electronic junctions. *Phys Chem Chem Phys* 2006;8(2):2572–90.